JOURNAL OF GUIDANCE, CONTROL, AND DYNAMICS
Vol. 30, No. 6, November–December 2007

Linearized Dynamics of Formation Flying Spacecraft on a J_2-Perturbed Elliptical Orbit

Jean-Francois Hamel* and Jean de Lafontaine†
Université de Sherbrooke, Sherbrooke, Quebec J1K 2R1, Canada

DOI: 10.2514/1.29438

A linearized set of equations of relative motion about a J_2-perturbed elliptical reference orbit is developed. This model uses analytical relations that are well suited for onboard applications. The inclusion of the J_2 perturbation in a simple analytical model can lead to formation flying guidance and control algorithms that make use of the natural J_2-induced relative motion to perform maneuvers instead of constantly compensating for this perturbation. The model uses the linearized differential drift rate of mean orbit elements to predict the impact of the J_2 perturbation on relative osculating spacecraft motion. It analytically provides the relative motion in Hill coordinates at any given true anomaly using only the initial osculating relative orbit elements and the initial orbit elements of the reference trajectory. A linear time-varying state-space form of the model is also presented. Simulation results show that relative motion prediction remains accurate over several orbits.

I. Introduction

FORMATION flying of spacecraft has been identified as a key technology for the 21st century. There is a trend toward replacing large expensive spacecraft with a group of smaller and cheaper spacecraft. Two of the main advantages of formation flying are reconfigurability and an increased robustness to system failures. The main drawback of formation flying spacecraft is an increased complexity of the complete system of spacecraft. This is particularly true for the guidance, navigation, and control system, for which the complexity grows rapidly with the number of spacecraft in the formation.

There is, however, at the same time, an increasing need for autonomy to decrease the cost of ground support. Ground support operations are a nonnegligible part of the cost of a mission, especially for small and low-cost scientific exploration missions. Therefore, the guidance and control system needs to perform autonomous decisions and tradeoffs in real time to decrease the tasks that need to be performed by the ground segment and make formation flying affordable. Moreover, to increase the robustness to single spacecraft failure, the guidance and control of the formation needs to be decentralized. This is especially challenging when the number of spacecraft in the formation becomes large.

Such guidance and control systems require accurate but simple models of reality in their algorithms. Models have to be accurate enough to prevent unnecessary fuel expenditure and simple enough to allow onboard implementation. If perturbation models are included in the onboard model of reality, natural motion induced by the perturbations can be used to support maneuvers. If these perturbations are not included, the guidance and control system will most likely compensate for these perturbations, therefore leading to an unnecessary fuel expenditure.

The most widely used relative orbital motion model is the Clohessy–Wiltshire–Hill model [1,2]. This model provides a time-explicit closed-form analytical solution to relative motion problem for circular unperturbed orbits. Lovell and Tragesser [3] reparametrized this model and demonstrated that the in-plane and out-of-plane nondrifting relative motion about a circular unperturbed orbit always follows an ellipse centered on the reference orbit, hence the name "football orbit."

However, assuming a circular reference orbit yields considerable errors when the eccentricity of the reference orbit grows [4]. Several models have therefore been proposed to model relative motion about unperturbed elliptical orbits [4–7]. In a recent publication, Lane and Axelrad [8] developed a time-explicit closed-form solution and studied the relative motion for bounded relative elliptical orbits. Melton [9] also proposed an alternative solution for small-eccentricity orbits.

Some models also take into account orbit perturbations. The most important perturbation encountered for the relative motion problem, and also the most studied, is the perturbation caused by the oblateness of the Earth, referred to as the J_2 perturbation. Schweighart and Sedwick [10,11] modified the classic Clohessy–Wiltshire–Hill model to include the orbit-averaged impact of the J_2 perturbation on a circular reference orbit.

The most challenging problem is to consider an elliptical and perturbed reference orbit. The most accurate way to model this problem is, of course, with numerical models [12,13]. In this case, solutions to the relative motion problem are obtained through numerical integration of the dynamics equations. However, numerical methods are not well suited for autonomous onboard applications because they typically require a lot of computing effort. Few publications actually provide an analytical solution to the relative motion around elliptical reference orbits that takes into account the J_2 perturbation.

Gim and Alfriend [14] solved the problem by proposing a state transition matrix that provides a time-explicit solution for the relative motion about a J_2-perturbed elliptical orbit. This model provides an accurate solution to the problem. However, even though the model is fully analytical, the elements of the state transition matrices remain quite complex, the states of the reference trajectory still need to be numerically computed, and matrix products and inversions remain. On the other hand, Schaub [5] studied the relative motion about elliptical reference orbits under J_2 perturbation with very simple expressions using classical orbit elements. However, this analysis is only performed in the mean orbit element space. This model cannot be written readily into a state transition matrix form, because the mapping between instantaneous, or osculating, orbit elements remains to be done.

The purpose of this paper is therefore to develop an analytical state transition matrix that accurately models relative motion about elliptical reference orbits under J_2 perturbation, while using simpler expressions and without the need to numerically propagate the states of the reference trajectory. It builds upon the approach of Schaub [5],

Received 22 December 2006; revision received 12 March 2007; accepted for publication 7 April 2007.

*Graduate Student, Department of Electrical Engineering. Student Member AIAA.
†Professor, Department of Electrical Engineering. Member AIAA.

but bridges the gap between osculating relative motion and relative mean orbit element drift. Desired formation relative dynamics will be described in terms of osculating, or actual, relative dynamics, which is why it is relevant to describe the relative motion in terms of osculating elements instead of mean elements. This simplified model is oriented toward an onboard implementation for mission scenarios in which computational power is limited, such as low-cost scientific missions.

The proposed model uses a geometric approach, similar to the work of Gim and Alfriend [14] but with certain simplifying assumptions. The model neglects variations in the short-period relative motion induced by the J_2 perturbation between the deputy and the chief, but includes osculating to mean orbit element mapping. In other words, it "adds" the relative mean orbit element drift to the natural osculating element Keplerian dynamics, neglecting the impact of short-period variations on the relative motion. This simplification is made at the cost of a prediction error as large as the short-period terms variations between the deputy and the chief. For two spacecraft orbiting very close to one another, this error will remain small because the short-period oscillations caused by the J_2 perturbation will be the same for both spacecraft. However, in all cases, this error will remain bounded even for long-term prediction. The main advantage of this approach is that the states of the reference trajectory at the true anomaly in which the relative dynamics need to be known are not required. All of the elements of the state transition matrix are computed from the initial position of the reference trajectory and the true anomaly for which the relative motion needs to be predicted. Models that take into account short-period variations [14] will need the states of the reference at the final time to do an accurate mapping between the mean elements and the osculating elements at this location.

The model presented here makes use of the classical orbit elements (singular if the reference orbit is circular). The main reason is that when the J_2 perturbation is modeled, the use of classical elements radically simplifies the expressions because only three of the six orbit elements experience secular drift. Obviously, the main drawback of the classical elements is that the model cannot be used for circular reference orbits. However, for missions with large-eccentricity orbits, such as ESA's currently planned Proba-3 mission, this model can be used without any fear of going through a singularity.

This paper is organized as follows. Section II presents a linear mapping between orbit elements and coordinates in the curvilinear Hill frame. Section III presents how the relative drift between the chief and the deputy can be modeled through the use of mean orbit elements. Section IV shows how the flight time can be estimated for a given true anomaly if the J_2 perturbation is considered. Then Sec. V combines those three results to yield a completely linearized set of equations describing the relative motion of spacecraft on a J_2-perturbed elliptical orbit. Section VI translates the model into a linear time-varying state-space model convenient for the design of control laws. Finally, Sec. VII presents simulation results and compares the accuracy of the model with the exact nonlinear model and the elliptical unperturbed model.

II. Linearized Mapping Between Hill Frame Coordinates and Orbit Elements

The linear mapping between the relative orbit elements and the coordinates in a local-vertical, local-horizontal (LVLH) Hill frame is realized by differentiating the position of a spacecraft with a given set of orbit elements in an inertial frame and then rotating this result in the Hill frame. This mapping has been already presented by Schaub [5,15] and is reproduced here using an alternative development, to serve as the starting point for the extension proposed here. A similar result, but with nonsingular elements, has also been obtained by Gim and Alfriend [14].

Let $\boldsymbol{e} = [a, e, i, \Omega, \omega, M]^T$ be the orbit element vector of a spacecraft, where a is the orbit semimajor axis, e is the orbit eccentricity, i is the orbit inclination, Ω is the right ascension of the ascending node, ω is the argument of perigee, and M is the mean anomaly. The Cartesian coordinates $\boldsymbol{r}^{\mathcal{I}}$ of the spacecraft in an Earth-centered inertial frame $\mathcal{I}$ can easily be obtained from $\boldsymbol{e}$:

$$\boldsymbol{r}^{\mathcal{I}} = r\begin{bmatrix} (\cos\Omega\cos\omega - \sin\Omega\sin\omega\cos i)\cos\nu - (\cos\Omega\sin\omega + \sin\Omega\cos\omega\cos i)\sin\nu \\ (\sin\Omega\cos\omega + \cos\Omega\sin\omega\cos i)\cos\nu + (-\sin\Omega\sin\omega + \cos\Omega\cos\omega\cos i)\sin\nu \\ \sin\omega\sin i\cos\nu + \cos\omega\sin i\sin\nu \end{bmatrix} \tag{1}$$

where ν is the true anomaly and r is the orbit radius:

$$r = \frac{a(1-e^2)}{1 + e\cos\nu} \tag{2}$$

Even though ν is not explicitly part of $\boldsymbol{e}$, it can be obtained iteratively from the mean anomaly and the orbit eccentricity through the well-known relations:

$$M = E - e\sin E \tag{3}$$

$$\tan\frac{\nu}{2} = \sqrt{\frac{1+e}{1-e}}\tan\frac{E}{2} \tag{4}$$

The impact on the inertial position of a small difference in orbit elements $\delta\boldsymbol{e} = [\delta a, \delta e, \delta i, \delta\Omega, \delta\omega, \delta M]^T$ can be estimated with a first-order approximation:

$$\Delta\boldsymbol{r}^{\mathcal{I}} = \frac{\partial\boldsymbol{r}^{\mathcal{I}}}{\partial r}\delta r + \frac{\partial\boldsymbol{r}^{\mathcal{I}}}{\partial\Omega}\delta\Omega + \frac{\partial\boldsymbol{r}^{\mathcal{I}}}{\partial\omega}\delta\omega + \frac{\partial\boldsymbol{r}^{\mathcal{I}}}{\partial i}\delta i + \frac{\partial\boldsymbol{r}^{\mathcal{I}}}{\partial\nu}\delta\nu \tag{5}$$

using [15]

$$\delta r = \frac{r}{a}\delta a + \frac{ae\sin\nu}{\eta}\delta M - a\cos\nu\delta e \tag{6}$$

$$\delta\nu = \frac{(1+e\cos\nu)^2}{\eta^3}\delta M + \frac{\sin\nu}{\eta^2}(2 + e\cos e)\delta e \tag{7}$$

where $\eta = \sqrt{1-e^2}$ leads to $\Delta\boldsymbol{r}^{\mathcal{I}}$ fully expressed as a function of $\boldsymbol{e}$ and $\delta\boldsymbol{e}$. The position increment can finally be expressed in a common LVLH Hill frame $\mathcal{H} = \{\hat{\boldsymbol{x}}, \hat{\boldsymbol{y}}, \hat{\boldsymbol{z}}\}$, where $\hat{\boldsymbol{x}}$ is a unit vector pointing in the direction of the spacecraft position $\boldsymbol{r}$ (Earth-centered position), $\hat{\boldsymbol{z}}$ is a unit vector normal to the orbital plane pointing in the direction of the orbit angular momentum, and $\hat{\boldsymbol{y}}$ completes the right-hand frame. To do so, the relative position of the spacecraft in the inertial frame is multiplied by the rotation matrix $C_{\mathcal{HI}}$ from $\mathcal{I}$ to $\mathcal{H}$:

$$\Delta\boldsymbol{r}^{\mathcal{H}} = \begin{bmatrix} x \\ y \\ z \end{bmatrix} = C_{\mathcal{HI}}\Delta\boldsymbol{r}^{\mathcal{I}} \tag{8}$$

where

$$C_{\mathcal{HI}} = \begin{bmatrix} \cos(\nu)\cos(\Omega) - \sin(\nu)\sin(\Omega)\cos(i) & \cos(\nu)\sin(\Omega) + \sin(\nu)\cos(\Omega)\cos(i) & \sin(\nu)\sin(i) \\ -\sin(\nu)\cos(\Omega) - \cos(\nu)\sin(\Omega)\cos(i) & -\sin(\nu)\sin(\Omega) + \cos(\nu)\cos(\Omega)\cos(i) & \cos(\nu)\sin(i) \\ \sin(\Omega)\sin(i) & -\cos(\Omega)\sin(i) & \cos(i) \end{bmatrix} \tag{9}$$

The final result is therefore the position of a deputy spacecraft in the Hill frame centered on a chief spacecraft as a function of the chief orbit elements $\boldsymbol{e}$ and the orbit element difference $\delta\boldsymbol{e}$ between the deputy and the chief:

$$x(\nu) = \frac{r}{a}\delta a - a\cos\nu\delta e + \frac{ae\sin\nu}{\eta}\delta M \tag{10}$$

$$y(\nu) = \frac{r\sin\nu(2 + e\cos\nu)}{\eta^2}\delta e + r\cos i\delta\Omega + r\delta\omega + \frac{r(1 + e\cos\nu)^2}{\eta^3}\delta M \tag{11}$$

$$z(\nu) = r\sin(\nu + \omega)\delta i - r\sin i\cos(\nu + \omega)\delta\Omega \tag{12}$$

III. Orbit Element Drift on a J_2-Perturbed Elliptical Orbit

If both orbits are Keplerian, setting $\delta a = 0$ ensures that both spacecraft have the same orbital period. This leads to a constant and nondrifting $\delta\boldsymbol{e}$. The prediction of relative motion can therefore be realized by sweeping ν from 0 to 2π in Eqs. (10–12) to get the relative motion for a complete orbit. However, if perturbations are encountered, $\delta\boldsymbol{e}$ will not remain constant. The orbit element differences will evolve with ν. If only the J_2 perturbation is considered, orbit elements will experience short-period oscillations and secular drift.

A common way to predict the effect of the J_2 perturbation on spacecraft motion is to use mean orbit element propagation. Mean orbit elements are orbit elements from which short-period oscillations have been removed. They only show secular drift, which can be easily expressed analytically.

Let $\bar{\boldsymbol{e}} = [\bar{a}, \bar{e}, \bar{i}, \bar{\Omega}, \bar{\omega}, \bar{M}]^T$ be the vector of mean orbit elements of the chief. It has been shown [16] that only $\bar{\Omega}$, $\bar{\omega}$, and $\bar{M}$ will have a nonzero secular drift rate caused by J_2:

$$\dot{\bar{a}} = 0 \tag{13}$$

$$\dot{\bar{e}} = 0 \tag{14}$$

$$\dot{\bar{i}} = 0 \tag{15}$$

$$\dot{\bar{\Omega}} = -\frac{3}{2}J_2\bar{n}\left(\frac{R_e}{\bar{p}}\right)^2\cos\bar{i} \tag{16}$$

$$\dot{\bar{\omega}} = \frac{3}{4}J_2\bar{n}\left(\frac{R_e}{\bar{p}}\right)^2(5\cos^2\bar{i} - 1) \tag{17}$$

$$\dot{\bar{M}} = \bar{n} + \frac{3}{4}J_2\bar{n}\left(\frac{R_e}{\bar{p}}\right)^2\bar{\eta}(3\cos^2\bar{i} - 1) \tag{18}$$

where $\bar{n}$ and $\bar{\eta}$ are, respectively, the mean motion and η computed with mean eccentricity; R_e is Earth's equatorial radius; and $\bar{p} = \bar{a}\bar{\eta}^2$ is the semilatus rectum based on mean orbit elements. A first-order mapping between actual elements (commonly referred to as *osculating*) and mean elements is provided by Schaub [15].

It is the difference in drift rates that is most relevant for formation flying because it has a long-term impact on the spacecraft relative motion. The impact of $\delta\boldsymbol{e}$ on those drift-rates differences can be approximated by differentiating the preceding equations:

$$\delta\dot{\bar{\Omega}} = \frac{\partial\dot{\bar{\Omega}}}{\partial\bar{a}}\delta\bar{a} + \frac{\partial\dot{\bar{\Omega}}}{\partial\bar{e}}\delta\bar{e} + \frac{\partial\dot{\bar{\Omega}}}{\partial\bar{i}}\delta\bar{i} \tag{19}$$

$$\delta\dot{\bar{\omega}} = \frac{\partial\dot{\bar{\omega}}}{\partial\bar{a}}\delta\bar{a} + \frac{\partial\dot{\bar{\omega}}}{\partial\bar{e}}\delta\bar{e} + \frac{\partial\dot{\bar{\omega}}}{\partial\bar{i}}\delta\bar{i} \tag{20}$$

$$\delta\dot{\bar{M}} = \frac{\partial\dot{\bar{M}}}{\partial\bar{a}}\delta\bar{a} + \frac{\partial\dot{\bar{M}}}{\partial\bar{e}}\delta\bar{e} + \frac{\partial\dot{\bar{M}}}{\partial\bar{i}}\delta\bar{i} \tag{21}$$

with the partial derivatives given by

$$\frac{\partial\dot{\bar{\Omega}}}{\partial\bar{a}} = \frac{21}{\bar{a}}C\cos\bar{i} \tag{22}$$

$$\frac{\partial\dot{\bar{\Omega}}}{\partial\bar{e}} = \frac{24\bar{e}}{\bar{\eta}^2}C\cos\bar{i} \tag{23}$$

$$\frac{\partial\dot{\bar{\Omega}}}{\partial\bar{i}} = 6C\sin\bar{i} \tag{24}$$

$$\frac{\partial\dot{\bar{\omega}}}{\partial\bar{a}} = -\frac{21}{2\bar{a}}C(5\cos^2\bar{i} - 1) \tag{25}$$

$$\frac{\partial\dot{\bar{\omega}}}{\partial\bar{e}} = \frac{12\bar{e}}{\bar{\eta}^2}C(5\cos^2\bar{i} - 1) \tag{26}$$

$$\frac{\partial\dot{\bar{\omega}}}{\partial\bar{i}} = -15C\sin(2\bar{i}) \tag{27}$$

$$\frac{\partial\dot{\bar{M}}}{\partial\bar{a}} = \frac{-3\bar{n}}{2\bar{a}} - \frac{\bar{\eta}}{4\bar{a}}C[63\cos(2\bar{i}) - 21] \tag{28}$$

$$\frac{\partial\dot{\bar{M}}}{\partial\bar{e}} = \frac{9\bar{e}}{\bar{\eta}}C(3\cos^2\bar{i} - 1) \tag{29}$$

$$\frac{\partial\dot{\bar{M}}}{\partial\bar{i}} = -9\bar{\eta}C\sin(2\bar{i}) \tag{30}$$

where

$$C \equiv \frac{J_2 \bar{n} R_e^2}{4p^2} \tag{31}$$

If the impact of relative short-period oscillations is neglected, it can be assumed that the evolution of the osculating orbit element differences will only be caused by the relative secular drift of mean orbit elements. Hence, the mean orbit element drift-rate difference is a way to estimate the orbit element differences of the drifting elements Ω, ω, and M:

$$\delta a(\tau) = \delta a_0 \tag{32}$$

$$\delta e(\tau) = \delta e_0 \tag{33}$$

$$\delta i(\tau) = \delta i_0 \tag{34}$$

$$\delta\Omega(\tau) = \delta\Omega_0 + \delta\dot{\bar{\Omega}}\tau \tag{35}$$

$$\delta\omega(\tau) = \delta\omega_0 + \delta\dot{\bar{\omega}}\tau \tag{36}$$

$$\delta M(\tau) = \delta M_0 + \delta\dot{\bar{M}}\tau \tag{37}$$

where $\delta a_0, \delta e_0, \delta i_0, \delta\Omega_0, \delta\omega_0$, and δM_0 are the initial osculating orbit element differences (at time t_0) and τ is the elapsed flight time since t_0.

IV. Estimation of the Flight Time

The evolution of the relative orbit elements is known as a function of the elapsed flight time. However, the proposed model needs to use only ν as an independent variable. Therefore, the flight time τ needs to be estimated as a function of the true anomaly ν.

The flight time can be estimated assuming that the evolution of mean anomaly with time is known. In an unperturbed environment, the mean anomaly rate is constant and equal to the mean motion n. However, in a J_2-perturbed environment, the mean anomaly rate is not equal to the mean motion. Neglecting the effect of short-period and long-period oscillations (thus only assuming secular drift) leads to Eq. (18). This assumption will leave short-period errors in the estimation of flight time, but will not cause any long-term drifting error for a J_2-perturbed orbit.

The relationship between eccentric anomaly E and mean anomaly M is the well-known Kepler equation:

$$M = E - e\sin E \tag{38}$$

where the eccentric anomaly can be expressed as a function of ν:

$$E = 2\arctan\left[\sqrt{\frac{1-e}{1+e}}\tan\left(\frac{\nu}{2}\right)\right] \tag{39}$$

Equations (38) and (39) can be used straightforwardly to get the estimated mean anomaly $M(\nu)$ for a given true anomaly ν. The elapsed time τ is obtained assuming a constant mean anomaly rate since t_0:

$$\tau = \frac{2\pi N_{\text{orb}} + M(\nu) - M_0}{\dot{\bar{M}}} \tag{40}$$

where N_{orb} is the number of orbits that the spacecraft has performed, if the model is to be used to perform long-term prediction over several orbits. This estimated flight time, combined with the estimated relative drift rate of orbit elements, allows the estimation of relative osculating elements as a function of the true anomaly.

The relevance of considering the J_2 perturbation in the evaluation of flight time can easily be demonstrated. Figure 1 shows the flight time estimation error if $a_0 = R_e + 1000$ km, $e_0 = 0.1$, $i_0 = \pi/4$, and $\Omega_0 = \omega_0 = M_0 = 0$ for a spacecraft evolving in a J_2-perturbed environment. The flight time estimation error is shown for 10 orbits. No secular error can be observed when considering the secular drift caused by J_2 on the mean anomaly rate. However if one assumes $\dot{M} = n$, the error reaches 100 s (nearly 1.5% of the orbital period) after 10 orbits and keeps growing. The short-period oscillations found in both cases are due to the neglected short-period J_2 perturbations.

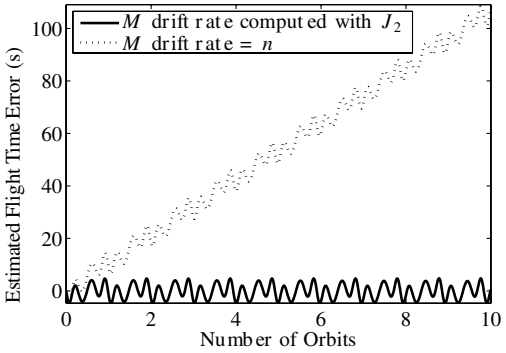

Fig. 1 Estimated flight time error.

V. Linearized Equations of Motion

The results of the previous sections can be combined to predict drifting spacecraft relative motion. Substituting δa, δe, δi, $\delta\Omega$, $\delta\omega$, and δM for $\delta a(\tau)$, $\delta e(\tau)$, $\delta i(\tau)$, $\delta\Omega(\tau)$, $\delta\omega(\tau)$, and $\delta M(\tau)$ and substituting $\boldsymbol{e}$ for $\boldsymbol{e}_0 + \dot{\bar{\boldsymbol{e}}}_0\tau$ into Eqs. (10–12) leads to a set of equations that takes into account the differential drift caused by J_2:

$$x(\nu) = \frac{r(\nu)}{a_0}\delta a_0 + \frac{a_0 e_0 \sin\nu}{\eta_0}(\delta M_0 + \delta\dot{\bar{M}}\tau) - a_0\cos\nu\delta e_0 \tag{41}$$

$$y(\nu) = \frac{r(\nu)\sin\nu(2 + e_0\cos\nu)}{\eta_0^2}\delta e_0 + r(\nu)\cos i_0(\delta\Omega_0 + \delta\dot{\bar{\Omega}}\tau) + r(\nu)(\delta\omega_0 + \delta\dot{\bar{\omega}}\tau) + \frac{r(\nu)(1 + e_0\cos\nu)^2}{\eta_0^3}(\delta M_0 + \delta\dot{\bar{M}}\tau) \tag{42}$$

$$z(\nu) = r(\nu)\sin(\nu + \omega_0 + \dot{\bar{\omega}}\tau)\delta i_0 - r(\nu)\sin i_0\cos(\nu + \omega_0 + \dot{\bar{\omega}}\tau)(\delta\Omega_0 + \delta\dot{\bar{\Omega}}\tau) \tag{43}$$

where $\boldsymbol{e}_0 = [a_0\ e_0\ i_0\ \Omega_0\ \omega_0\ M_0]^T$ are the osculating orbit elements of the reference orbit and $\dot{\bar{\boldsymbol{e}}}_0 = [0\ 0\ 0\ \dot{\bar{\Omega}}\ \dot{\bar{\omega}}\ \dot{\bar{M}}]^T$ are the corresponding mean element drift rates.

Even though Eqs. (41–43) may appear to be simplistic statements at first, they in fact represent the crux of the advantage of the main assumption upon which this model is built. The $\delta\Omega_0$, $\delta\omega_0$, and δM_0 terms are osculating relative orbit elements, whereas $\delta\dot{\bar{\Omega}}$, $\delta\dot{\bar{\omega}}$, and $\delta\dot{\bar{M}}$ are mean relative orbit element drift rates. This assumes that relative motion between osculating elements only shows secular drift and no short-period oscillations. This will, of course, lead to an inevitable bounded prediction error in the model, but all of the terms of Eqs. (41–43) can be expressed only from osculating relative orbit elements and initial osculating orbit elements of the reference trajectory, thus avoiding the need to numerically propagate the states of the chief.

For this to be realized, $\delta\dot{\bar{\Omega}}$, $\delta\dot{\bar{\omega}}$, and $\delta\dot{\bar{M}}$ (currently functions of $\delta\bar{a}$, $\delta\bar{e}$, and $\delta\bar{i}$) need to be expressed as a linear function of the osculating element differences. This can be done by studying the mapping function $\bar{\boldsymbol{e}} = \xi\boldsymbol{e}$ between the mean and osculating elements. The matrix $\partial\xi/\partial\boldsymbol{e}$ is approximately an identity matrix with off-diagonal terms of the order of J_2 or smaller [15]. It is thus reasonable to assume

that a small increment of an osculating orbit element will cause the same change of the corresponding mean element. However, it has been noted that this assumption is not valid for $\bar{a}$, for which the off-diagonal terms are nonnegligible. Therefore, $\delta\bar{a}$ has to be approximated with a linearization of the function $\bar{a} = \xi_a \boldsymbol{e}$. Schaub [15] provides a first-order mapping between osculating and mean elements that can be used to approximate $\delta\bar{a}$:

$$\bar{a} = \xi_a = a - a\frac{J_2}{2}\left(\frac{R_e}{a}\right)^2\left\{(3\cos^2 i - 1)\left[\left(\frac{a}{r}\right)^3 - \frac{1}{\eta^3}\right] + 3(1-\cos^2 i)\left(\frac{a}{r}\right)^3 \cos(2\omega + 2\nu)\right\} \tag{44}$$

This function can be linearized about the orbit $\boldsymbol{e}$:

$$\delta\bar{a} = \frac{\partial\xi_a}{\partial a}\delta a + \frac{\partial\xi_a}{\partial e}\delta e + \frac{\partial\xi_a}{\partial i}\delta i + \frac{\partial\xi_a}{\partial\omega}\delta\omega + \frac{\partial\xi_a}{\partial\nu}\delta\nu \tag{45}$$

with $\delta\nu$ given by Eq. (7). The analytical expressions of the partial derivatives in Eq. (45) are developed in Appendix A.

The relative velocity can be obtained straightforwardly by differentiating Eqs. (41–43) with respect to time and taking $\dot{\tau} = 1$. For that purpose, only r, ν, Ω, ω, M, and τ are considered to be functions of time:

$$\dot{x}(\nu) = \frac{\dot{r}}{a_0}\delta a_0 + \frac{a_0 e_0 \dot{\nu}\cos\nu}{\eta_0}(\delta M_0 + \delta\dot{\bar{M}}\tau) + \frac{a_0 e_0 \sin\nu}{\eta_0}\delta\dot{\bar{M}} + a_0\dot{\nu}\sin\nu\,\delta e_0 \tag{46}$$

$$\begin{aligned}\dot{y}(\nu) = {} & \frac{1}{\eta_0^2}[\dot{r}\sin\nu(2 + e_0\cos\nu) + r\dot{\nu}(2 + e_0\cos\nu)\cos\nu \\ & - re_0\dot{\nu}\sin^2\nu] + \dot{r}\cos i_0(\delta\Omega_0 + \delta\dot{\bar{\Omega}}\tau) + r\cos i_0\delta\dot{\bar{\Omega}} \\ & + \dot{r}(\delta\omega_0 + \delta\dot{\bar{\omega}}\tau) + r\delta\dot{\bar{\omega}} + \frac{1}{\eta_0^3}[\dot{r}(1 + e_0\cos\nu)^2(\delta M_0 + \delta\dot{\bar{M}}\tau) \\ & - 2re_0\dot{\nu}\sin\nu(1 + e_0\cos\nu)(\delta M_0 + \delta\dot{\bar{M}}\tau) \\ & + r(1 + e_0\cos\nu)^2\delta\dot{\bar{M}}]\end{aligned} \tag{47}$$

$$\begin{aligned}\dot{z}(\nu) = {} & \dot{r}\sin(\nu + \omega_0 + \dot{\bar{\omega}}\tau)\delta i_0 - r\cos(\nu + \omega_0 + \dot{\bar{\omega}}\tau)(\dot{\nu} + \dot{\bar{\omega}})\delta i_0 \\ & - \dot{r}\cos(\nu + \omega_0 + \dot{\bar{\omega}}\tau)\sin i_0(\delta\Omega_0 + \delta\dot{\bar{\Omega}}\tau) \\ & + r\sin(\nu + \omega_0 + \dot{\bar{\omega}}\tau)(\dot{\nu} + \dot{\bar{\omega}})\sin i_0(\delta\Omega_0 + \delta\dot{\bar{\Omega}}\tau) \\ & - r\cos(\nu + \omega_0 + \dot{\bar{\omega}}\tau)\sin i_0\delta\dot{\bar{\Omega}}\end{aligned} \tag{48}$$

where

$$\dot{r}(\nu) = \frac{a_0 e_0 \sin\nu}{\eta}\dot{\bar{M}} \tag{49}$$

$$\dot{\nu}(\nu) = \frac{(1 + e_0\cos\nu)^2}{\eta^3}\dot{\bar{M}} \tag{50}$$

Collecting Eqs. (41–48) and substituting $\delta\dot{\bar{\Omega}}$, $\delta\dot{\bar{\omega}}$, $\delta\dot{\bar{M}}$, $\delta\bar{a}$, $\delta\bar{e}$, and $\delta\bar{i}$ by their equivalent function of the initial reference orbit $\boldsymbol{e}_0$ and initial offset $\delta\boldsymbol{e}_0$ leads to a very convenient way of expressing the model:

$$\delta\boldsymbol{X}(\nu) = \Phi(\boldsymbol{e}_0, \nu)\delta\boldsymbol{e}_0 \tag{51}$$

where $\delta\boldsymbol{X} = [\dot{x}\ \dot{y}\ \dot{z}\ x\ y\ z]^T$. The elements of Φ are given in Appendix B. Given an initial reference orbit $\boldsymbol{e}_0$, the relative dynamics of a spacecraft with a small orbit element offset $\delta\boldsymbol{e}_0$ can be predicted through analytical equations for any point of the orbit ν considering a J_2-perturbed orbit.

In summary, the steps required to predict the relative motion are as follows:

1) Define the initial reference orbit state vector $\boldsymbol{e}_0$ and the true anomaly ν for which the formation is needed.

2) Translate $\boldsymbol{e}_0$ into the mean orbit element space [15]: $\bar{\boldsymbol{e}}_0 = \xi\boldsymbol{e}_0$.

3) Compute the mean reference orbit element drift with Eqs. (13–18) from $\bar{\boldsymbol{e}}_0$.

4) Compute the mean orbit element drift-rate partial derivatives at $\bar{\boldsymbol{e}}_0$ [Eqs. (22–30)].

5) Compute the ξ_a partial derivatives at $\boldsymbol{e}_0$ with the results of Appendix A.

6) Estimate the flight time τ at ν from Eqs. (38–40).

7) Compute the elements of the matrix $\Phi(\boldsymbol{e}_0, \nu)$ found in Appendix B.

The relative Hill coordinates $\delta\boldsymbol{X}(\nu)$ for any initial relative position $\delta\boldsymbol{e}_0$ can then be obtained through $\delta\boldsymbol{X} = \Phi(\boldsymbol{e}_0, \nu)\delta\boldsymbol{e}_0$. Assuming Φ is nonsingular, the model can also be numerically inverted to provide the initial required orbit element differences given a desired configuration at a specific point ν of the orbit:

$$\delta\boldsymbol{e}_0 = [\Phi(\boldsymbol{e}_0, \nu)]^{-1}\delta\boldsymbol{X}(\nu) \tag{52}$$

This result is useful in the sense that it provides the current $\delta\boldsymbol{e}_0$ required to reach, without any further control effort, a desired formation $\delta\boldsymbol{X}$ at a point ν, considering all spacecraft are under the influence of the J_2 perturbation. The difference between the result of Eq. (52) and the actual orbit element differences represent the maneuver that is to be performed to achieve the formation $\delta\boldsymbol{X}$ at the desired true anomaly but following natural motion.

The matrix Φ will become singular as eccentricity e tends toward zero, because a ω or an M offset cannot be differentiated for a perfectly circular orbit. Furthermore, when e is close to zero, ω can move very quickly around the orbit, which means that large $\delta\omega$, far beyond the validity limit of the linearized model, can be encountered. The model also fails if $i = 0$ because Ω cannot be defined.

For circular orbits, the J_2 linearized model of Schweighart and Sedwick [10,11] is better suited to predict relative motion. For the zero-inclination case, an unperturbed model would prove to be sufficiently accurate because equatorial orbits are weakly affected by the J_2 perturbation, which can approximately be modeled by an equivalent increased gravity in this case. This model would need to use a different set of elements, such as the equinoctial elements, because Ω cannot be defined for an equatorial orbit.

VI. State-Space Model

The results of Sec. V can also be expressed in a time-varying linear state-space dynamic model of the form

$$\delta\dot{\boldsymbol{e}} = A(\boldsymbol{e}_c)\delta\boldsymbol{e} + B(\boldsymbol{e}_c)\boldsymbol{u} \tag{53}$$

where $\boldsymbol{e}_c = [a_c\ e_c\ i_c\ \Omega_c\ \omega_c\ M_c]^T$ is the orbit element vector of the reference, or the *chief* (that can be any element of the formation or simply a virtual point in space), and $\delta\boldsymbol{e}$ is the orbit element offset with respect to the reference. The control vector $\boldsymbol{u}$ is composed of the radial control acceleration u_r, the transverse control acceleration u_θ, and out-of-plane control acceleration u_h, such that

$$\boldsymbol{u} = \begin{bmatrix} u_r \\ u_\theta \\ u_h \end{bmatrix} \tag{54}$$

Assuming the chief follows a J_2-perturbed uncontrolled motion, the matrix A depicts the relative drift of the orbit element caused by the natural J_2 perturbation, whereas the B matrix links the deputy control accelerations to its relative orbit element dynamics.

Because only Ω, ω, and M will experience relative drift, the matrix A is filled by expanding Eqs. (19–21):

$$A = \begin{bmatrix} 0 & 0 & 0 & 0 & 0 & 0 \\ 0 & 0 & 0 & 0 & 0 & 0 \\ 0 & 0 & 0 & 0 & 0 & 0 \\ \frac{\partial\dot{\Omega}}{\partial a}\frac{\partial\xi_a}{\partial a} & \frac{\partial\dot{\Omega}}{\partial a}\frac{\partial\xi_a}{\partial e} + \frac{\partial\dot{\Omega}}{\partial e} + \frac{\partial\dot{\Omega}}{\partial a}\frac{\partial\xi_a}{\partial \nu}\frac{\sin\nu_c}{\eta_c^2} & \frac{\partial\dot{\Omega}}{\partial a}\frac{\partial\xi_a}{\partial i} + \frac{\partial\dot{\Omega}}{\partial i} & 0 & \frac{\partial\dot{\Omega}}{\partial a}\frac{\partial\xi_a}{\partial \omega} & \frac{\partial\dot{\Omega}}{\partial a}\frac{\partial\xi_a}{\partial \nu}\frac{(1+e_c\cos\nu_c)^2}{\eta_c^3} \\ \frac{\partial\dot{\omega}}{\partial a}\frac{\partial\xi_a}{\partial a} & \frac{\partial\dot{\omega}}{\partial a}\frac{\partial\xi_a}{\partial e} + \frac{\partial\dot{\omega}}{\partial e} + \frac{\partial\dot{\omega}}{\partial a}\frac{\partial\xi_a}{\partial \nu}\frac{\sin\nu_c}{\eta_c^2} & \frac{\partial\dot{\omega}}{\partial a}\frac{\partial\xi_a}{\partial i} + \frac{\partial\dot{\omega}}{\partial i} & 0 & \frac{\partial\dot{M}}{\partial a}\frac{\partial\xi_a}{\partial \omega} & \frac{\partial\dot{M}}{\partial a}\frac{\partial\xi_a}{\partial \nu}\frac{(1+e_c\cos\nu_c)^2}{\eta_c^3} \\ \frac{\partial\dot{M}}{\partial a}\frac{\partial\xi_a}{\partial a} & \frac{\partial\dot{M}}{\partial a}\frac{\partial\xi_a}{\partial e} + \frac{\partial\dot{M}}{\partial e} + \frac{\partial\dot{M}}{\partial a}\frac{\partial\xi_a}{\partial \nu}\frac{\sin\nu_c}{\eta_c^2} & \frac{\partial\dot{M}}{\partial a}\frac{\partial\xi_a}{\partial i} + \frac{\partial\dot{M}}{\partial i} & 0 & \frac{\partial\dot{M}}{\partial a}\frac{\partial\xi_a}{\partial \omega} & \frac{\partial\dot{M}}{\partial a}\frac{\partial\xi_a}{\partial \nu}\frac{(1+e_c\cos\nu_c)^2}{\eta_c^3} \end{bmatrix} \tag{55}$$

The B matrix is made of the terms of the well-known Gauss variational equations (GVEs) [15]. The GVEs relate the impact of a perturbation or control acceleration on each of the orbit elements. Thus, the elements of the B matrix are

$$B = \begin{bmatrix} \frac{2a_c^2 e_c \sin\nu_c}{h_c} & \frac{2a_c^2 p_c}{r_c} & 0 \\ \frac{p_c \sin\nu_c}{h_c} & \frac{(p_c+r_c)\cos r_c + r_c e_c}{h_c} & 0 \\ 0 & 0 & \frac{r_c\cos(\nu_c+\omega_c)}{h_c} \\ 0 & 0 & \frac{r_c\sin(\nu_c+\omega_c)}{h_c \sin i_c} \\ -\frac{p_c\cos\nu_c}{h_c e_c} & \frac{(p_c+r_c)\sin\nu_c}{h_c e_c} & -\frac{r_c\sin(\nu_c+\omega_c)\cos i_c}{h_c \sin i_c} \\ -\frac{b_c p_c\cos\nu - 2r_c e_c}{a_c h_c e_c} & -(p_c + r_c)\sin\nu_c & 0 \end{bmatrix} \tag{56}$$

where $p_c = a_c(1 - e_c^2)$ is the semilatus rectum of the chief's orbit, $h_c = \sqrt{\mu p_c}$ is the reference orbit's angular momentum (with μ being Earth's gravitational parameter), and $b_c = a_c\sqrt{1 - e_c^2}$ is the reference orbit's semiminor axis. This linear time-varying, or more accurately "chief orbit element-varying," state-space form will accurately model the secular relative drift caused by J_2 on an eccentric orbit, but fails to model the relative short-period oscillations between the chief and the deputy caused by the J_2 perturbation. Nevertheless, this linear model could prove to be useful in the design of control systems that make use of linear time-varying state-space models, such as model-predictive controllers or gain-scheduling controllers.

VII. Simulation Results

The accuracy of the closed-form solution [Eqs. (41–43) and (46–48)] was evaluated with respect to the "true" relative dynamics, based on numerical integration of J_2-perturbed dynamics. This accuracy is also compared with the accuracy of the elliptical linearized equations of unperturbed elliptical motion [8], referred to as the unperturbed elliptical motion model. The chief orbit elements $\boldsymbol{e}_0$ were set to a slightly elliptical 45-deg inclined low-Earth orbit, as described in Table 1. The deputy was given a small orbit element offset $\delta\boldsymbol{e}_0$, as shown in Table 2. Only δa_0 was set to zero. The reason is that in an unperturbed environment, this condition is sufficient to ensure nondrifting relative motion. However, in a J_2-perturbed environment, the nondrifting conditions are slightly different [17]. Therefore, those conditions lead to a secular relative drift that a set of equations that does not include the J_2 perturbation will not be able to model. The resulting relative position in a J_2-perturbed environment, obtained with numerical integration, is presented in Fig. 2, and Fig. 3 shows the resulting relative velocity.

Table 1 Chief initial orbit elements

$\boldsymbol{e}_0$	
a_0	$1.1R_e$
e_0	0.05
i_0	$\pi/4$
Ω_0	0.1
ω_0	0.1
M_0	0.1

Table 2 Deputy initial orbit element offset

$\delta\boldsymbol{e}_0$	
δa_0	0
δe_0	+0.0001
δi_0	+0.0001
$\delta\Omega_0$	−0.0001
$\delta\omega_0$	−0.0001
δM_0	+0.0001

Figure 4 shows the relative position error between the predicted and the true curvilinear Hill frame coordinates for both models (perturbed and unperturbed) for 10 orbital periods. As expected, the unperturbed elliptical motion model cannot predict the relative drift caused by the J_2 perturbation and shows a growing relative error in x, y, and z. On the other hand, the model developed here, which includes the J_2 perturbation through relative mean orbit element differences, does not show any secularly growing error and accurately models the long-term effect of J_2. The short-period variations of the position errors are mainly due to the neglected relative short-period motion between the chief and the deputy. This error is bounded within 1.5% of the maximum relative position at any point in time on all three axes. Therefore, only other perturbations, such as other gravitational harmonics, solar radiation pressure, or

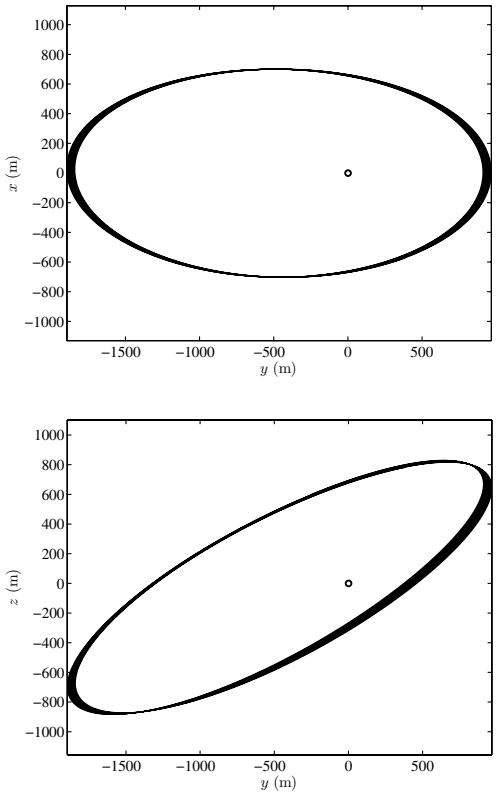

Fig. 2 In-plane (top) and out-of-plane (bottom) deputy relative motion in Hill frame for 10 orbits in a J_2-perturbed environment.

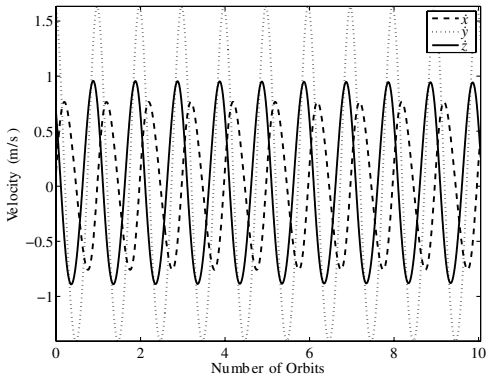

Fig. 3 Relative velocity in Hill frame for 10 orbits in a J_2-perturbed environment.

atmospheric drag would affect the long-term accuracy of the model. With the linearized elliptical model, the error grows by approximately 1% per orbit, reaching nearly 13% after 10 orbits on the x, y, and z axes. The same conclusions can be drawn for velocity (Figs. 3 and 5). Only short-period perturbations affect the $\dot{x}$, $\dot{y}$, and $\dot{z}$ errors.

VIII. Conclusions

A linearized analytical set of equations that provides the position and velocity of a deputy orbiting close to a chief on a J_2-perturbed elliptical orbit was developed. This model provides a simpler state transition matrix for relative motion by assuming that relative motion in osculating coordinates is only caused by relative mean orbit element drift. The model uses the linearized drift-rate difference of the mean orbit element difference to predict the relative secular drift caused by J_2. It was proven to accurately model the secular drift caused by J_2, leaving only errors caused by short-period relative motion between the chief and the deputy. It was shown that even though simplifications were made, only a bounded prediction error remains, even for long-term prediction. This error is bounded by the size of the relative motion induced by short-period J_2 perturbation terms.

The model provides the position and velocity of a deputy orbiting near a chief spacecraft for any point of the orbit, only from the relative orbit element vector and the initial state vector of the chief. The model avoids the need to numerically propagate the states of the chief forward in time. The model can be numerically inverted to yield the current required orbit element differences to reach a desired formation (described as position and velocity in Hill coordinates) at a specific true anomaly. The consideration of the J_2 perturbation in the model allows the use of the model several orbits in advance, because virtually no secular drift error caused by J_2 remains. Only errors caused by other perturbations, such as other gravitational field harmonics (J_3, J_4, etc.), solar radiation pressure, or differential drag will affect the long-term modeling accuracy of the model. A linear time-varying state-space expression of the model was also presented.

This model would be particularly well suited for onboard guidance and control applications, because the analytical equations require no numerical iteration to predict the relative motion once the initial mean and osculating orbit elements of the chief are known. The naturally induced secular relative motion by the J_2 perturbation is included in the model and can therefore be used to perform maneuvers. Furthermore, once the analytically defined Φ matrix is known, the relative motion of any spacecraft of the formation can be obtained with only one matrix multiplication, $\Phi\delta\boldsymbol{e}$. The same matrix Φ can be used for all of the spacecraft of the formation, assuming the relative orbit elements are sufficiently small. The only information required is the relative orbit elements of the spacecraft in the formation. This approach would prove to be increasingly efficient as the number of spacecraft of the formation becomes large.

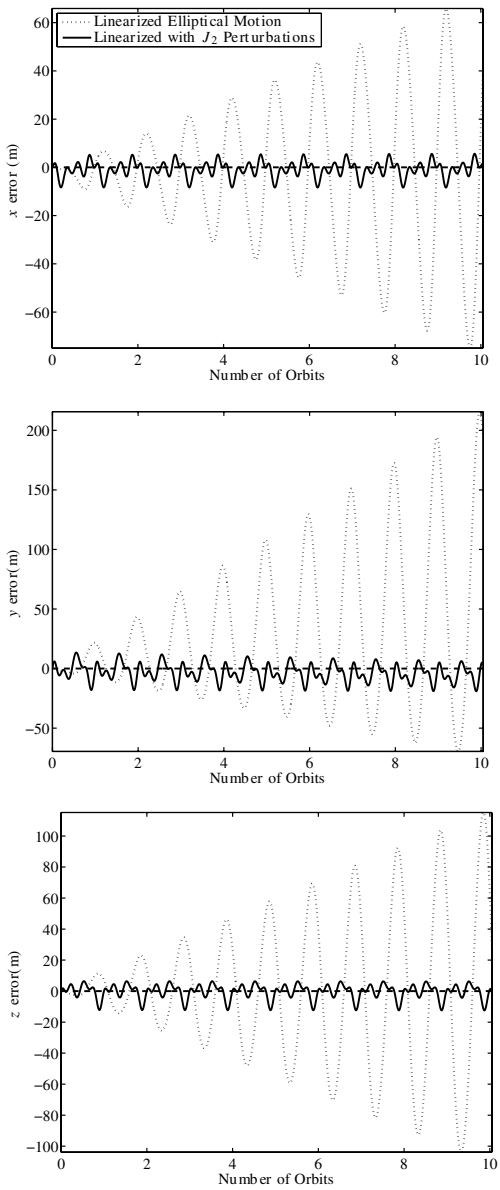

Fig. 4 Position modeling error for the linearized elliptical motion model and the linearized elliptical motion considering the J_2 perturbation in a J_2-perturbed environment.

To simplify the terms of the state transition matrix, classical orbit elements are used. Thus, the model can only be applied to noncircular and inclined orbits. For circular or equatorial orbits, some of the classical orbit elements used in this model are not defined. For both cases, previously existing models can be used or an extension to nonsingular orbit elements could also be implemented.

Appendix A: Linearization of the Osculating to Mean Orbit Element Mapping Function

The function [15]

$$\bar{a} = \xi_a = a - a\gamma_2\left\{(3\cos^2 i - 1)\left[\left(\frac{a}{r}\right)^3 - \frac{1}{\eta^3}\right] + 3(1-\cos^2 i)\left(\frac{a}{r}\right)^3 \cos(2\omega + 2\nu)\right\} \tag{A1}$$

where

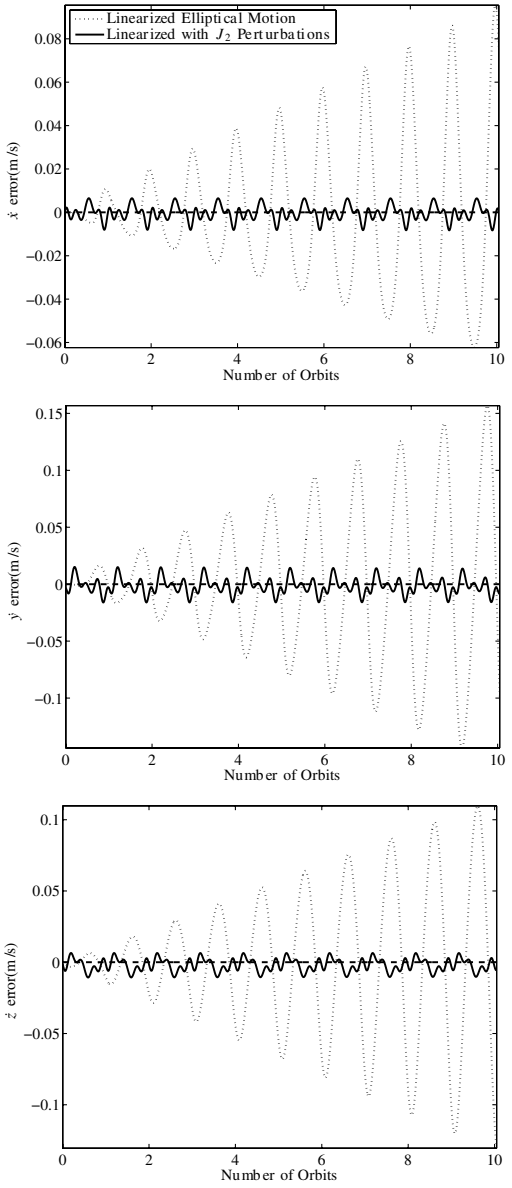

Fig. 5 Velocity modeling error for the linearized elliptical motion model and the linearized elliptical motion considering the J_2 perturbation in a J_2-perturbed environment.

$$\gamma_2 = -\frac{J_2}{2}\left(\frac{R_e}{a}\right)^2 \tag{A2}$$

can be linearized about $\boldsymbol{e}$ to provide an approximation of the mean semimajor axis increment from the osculating orbit element difference $\delta\boldsymbol{e}$:

$$\delta\bar{a} = \frac{\partial\xi_a}{\partial a}\delta a + \frac{\partial\xi_a}{\partial e}\delta e + \frac{\partial\xi_a}{\partial i}\delta i + \frac{\partial\xi_a}{\partial\omega}\delta\omega + \frac{\partial\xi_a}{\partial\nu}\left(\frac{(1+e\cos\nu)^2}{\eta^3}\delta M + \frac{\sin\nu}{\eta^2}\delta e\right) \tag{A3}$$

where ν_0 is the initial true anomaly of the chief. The partial derivatives are

$$\frac{\partial\xi_a}{\partial a} = 1 - \gamma_2\left\{(3\cos^2 i - 1)\left[\left(\frac{a}{r}\right)^3 - \frac{1}{\eta^3}\right] + 3(1-\cos^2 i)\left(\frac{a}{r}\right)^3\cos(2\omega+2\nu)\right\} \approx 1 \tag{A4}$$

$$\frac{\partial\xi_a}{\partial e} = a\gamma_2\left\{[2-3(\sin i)^2]\left(3\frac{(1+e\cos\nu)^2\cos\nu}{\eta^6} + 6\frac{(1+e\cos\nu)^3 e}{\eta^8} - 3\frac{e}{\eta^5}\right) + 9\frac{\sin^2 i(1+e\cos\nu)^2\cos(2w+2\nu)\cos\nu}{\eta^6} + 18\frac{\sin^2 i(1+e\cos\nu)^3\cos(2w+2\nu)e}{\eta^8}\right\} \tag{A5}$$

$$\frac{\partial\xi_a}{\partial i} = -3a\gamma_2\sin(2i)\left\{\left(\frac{a}{r}\right)^3[1-\cos(2\omega+2\nu)] - \frac{1}{\eta^3}\right\} \tag{A6}$$

$$\frac{\partial\xi_a}{\partial\omega} = -6a\gamma_2(1-\cos^2 i)\left(\frac{a}{r}\right)^3\sin(2\omega+2\nu) \tag{A7}$$

$$\frac{\partial\xi_a}{\partial\nu} = a\gamma_2\frac{(1+e\cos\nu)^2}{\eta^6}[(-9\cos^2 i+3)e\sin\nu - (9-9\cos^2 i)\cos(2\omega+2\nu)e\sin\nu - (6-6\cos^2 i)(1+e\cos\nu)\sin(2\omega+2\nu)] \tag{A8}$$

Appendix B: Φ Matrix

This Appendix presents the elements of a matrix Φ defined as

$$\begin{bmatrix}\dot{x}\\ \dot{y}\\ \dot{z}\\ x\\ y\\ z\end{bmatrix} = \Phi(\boldsymbol{e}_0,\nu)\begin{bmatrix}\delta a_0\\ \delta e_0\\ \delta i_0\\ \delta\Omega_0\\ \delta\omega_0\\ \delta M_0\end{bmatrix}$$

where $\boldsymbol{e}_0$ is the initial orbit element vector of the chief and ν is the true anomaly for which the formation is needed. The elements of Φ are obtained by collecting Eqs. (41–43) and (46–48) and by using the definition of mean orbit element drift of Eqs. (16–18), the partial derivatives of Eqs. (22–30) and of Appendix A, and the estimated flight time τ of Eq. (40).

The elements of Φ for the computation of $\dot{x}$ are

$$\kappa_{\dot{x}} = \frac{a_0 e_0\dot{\nu}\cos\nu}{\eta_0}$$

$$\Phi_{11} = \frac{\dot{r}}{a_0} + \left(\kappa_{\dot{x}}\tau + \frac{a_0 e_0\sin\nu}{\eta_0}\right)\frac{\partial\dot{\bar{M}}}{\partial\bar{a}}$$

$$\Phi_{12} = \left(\kappa_{\dot{x}}\tau + \frac{a_0 e_0\sin\nu}{\eta_0}\right)\left[\frac{\partial\dot{\bar{M}}}{\partial\bar{a}}\frac{\partial\xi_a}{\partial e} + \frac{\partial\dot{\bar{M}}}{\partial\bar{a}}\frac{\partial\xi_a}{\partial\nu}\frac{\sin\nu_0}{\eta_0^2}(2+e_0\cos e_0)\right]$$

$$\Phi_{13} = \left(\kappa_{\dot{x}}\tau + \frac{a_0 e_0\sin\nu}{\eta_0}\right)\left(\frac{\partial\dot{\bar{M}}}{\partial\bar{a}}\frac{\partial\xi_a}{\partial i} + \frac{\partial\dot{\bar{M}}}{\partial\bar{i}}\right)$$

$$\Phi_{14} = 0$$

$$\Phi_{15} = \left(\kappa_{\dot{x}}\tau + \frac{a_0 e_0\sin\nu}{\eta_0}\right)\frac{\partial\dot{\bar{M}}}{\partial\bar{a}}\frac{\partial\xi_a}{\partial\omega}$$

$$\Phi_{16} = \kappa_{\dot{x}} + \left(\kappa_{\dot{x}}\tau + \frac{a_0 e_0\sin\nu}{\eta_0}\right)\frac{\partial\dot{\bar{M}}}{\partial\bar{a}}\frac{\partial\xi_a}{\partial\nu}\frac{(1+e_0\cos\nu_0)^2}{\eta_0^3}$$

The elements of Φ for the computation of $\dot{y}$ are

$$\kappa_{\dot{y}} = \frac{\dot{r}(1+e_0\cos\nu)^2}{\eta_0^3} - \frac{2e_0\dot{\nu}(1+e_0\cos\nu)\sin\nu}{\eta_0^3}$$

$$\Phi_{21} = (\dot{r}\cos i_0\tau + r\cos i_0)\frac{\partial\dot{\bar{\Omega}}}{\partial\bar{a}} + (\dot{r}\tau + r)\frac{\partial\dot{\bar{\omega}}}{\partial\bar{a}} + \left[\kappa_{\dot{y}}\tau + \frac{r(1+e_0\cos\nu)^2}{\eta_0^3}\right]\frac{\partial\dot{\bar{M}}}{\partial\bar{a}}$$

$$\Phi_{22} = \frac{1}{\eta_0^2}[r\dot{\nu}\cos\nu(2+e_0\cos\nu) - re_0\dot{\nu}\sin^2\nu + \dot{r}\sin\nu(2+e_0\cos\nu)] + (\dot{r}\cos i_0\tau + r\cos i_0) \times \left[\frac{\partial\dot{\bar{\Omega}}}{\partial\bar{a}}\frac{\partial\xi_a}{\partial e} + \frac{\partial\dot{\bar{\Omega}}}{\partial\bar{a}}\frac{\partial\xi_a}{\partial\nu}\frac{\sin\nu_0}{\eta_0^2}(2+e_0\cos e_0) + \frac{\partial\dot{\bar{\Omega}}}{\partial\bar{e}}\right] + (\dot{r}\tau + r)\left[\frac{\partial\dot{\bar{\omega}}}{\partial\bar{a}}\frac{\partial\xi_a}{\partial e} + \frac{\partial\dot{\bar{\omega}}}{\partial\bar{a}}\frac{\partial\xi_a}{\partial\nu}\frac{\sin\nu_0}{\eta_0^2}(2+e_0\cos e_0) + \frac{\partial\dot{\bar{\omega}}}{\partial\bar{e}}\right] + \left[\kappa_{\dot{y}}\tau + \frac{r(1+e_0\cos\nu)^2}{\eta_0^3}\right]\left[\frac{\partial\dot{\bar{M}}}{\partial\bar{a}}\frac{\partial\xi_a}{\partial e} + \frac{\partial\dot{\bar{M}}}{\partial\bar{a}}\frac{\partial\xi_a}{\partial\nu}\frac{\sin\nu_0}{\eta_0^2}(2+e_0\cos e_0) + \frac{\partial\dot{\bar{M}}}{\partial\bar{e}}\right]$$

$$\Phi_{23} = (\dot{r}\cos i_0\tau + r\cos i_0)\left(\frac{\partial\dot{\bar{\Omega}}}{\partial\bar{a}}\frac{\partial\xi_a}{\partial i} + \frac{\partial\dot{\bar{\Omega}}}{\partial\bar{i}}\right) + (\dot{r}\tau + r)\left(\frac{\partial\dot{\bar{\omega}}}{\partial\bar{a}}\frac{\partial\xi_a}{\partial i} + \frac{\partial\dot{\bar{\omega}}}{\partial\bar{i}}\right) + \left[\kappa_{\dot{y}}\tau + \frac{r(1+e_0\cos\nu)^2}{\eta_0^3}\right]\left(\frac{\partial\dot{\bar{M}}}{\partial\bar{a}}\frac{\partial\xi_a}{\partial i} + \frac{\partial\dot{\bar{M}}}{\partial\bar{i}}\right)$$

$$\Phi_{24} = \dot{r}\cos i_0$$

$$\Phi_{25} = \dot{r} + (\dot{r}\cos i_0\tau + r\cos i_0)\frac{\partial\dot{\bar{\Omega}}}{\partial\bar{a}}\frac{\partial\xi_a}{\partial\omega} + (\dot{r}\tau + r)\frac{\partial\dot{\bar{\omega}}}{\partial\bar{a}}\frac{\partial\xi_a}{\partial\omega} + \left[\kappa_{\dot{y}}\tau + \frac{r(1+e_0\cos\nu)^2}{\eta_0^3}\right]\frac{\partial\dot{\bar{M}}}{\partial\bar{a}}\frac{\partial\xi_a}{\partial\omega}$$

$$\Phi_{26} = \kappa_{\dot{y}} + (\dot{r}\cos i_0\tau + r\cos i_0)\frac{\partial\dot{\bar{\Omega}}}{\partial\bar{a}}\frac{\partial\xi_a}{\partial\nu}\frac{(1+e_0\cos\nu_0)^2}{\eta_0^3} + (\dot{r}\tau + r)\frac{\partial\dot{\bar{\omega}}}{\partial\bar{a}}\frac{\partial\xi_a}{\partial\nu}\frac{(1+e_0\cos\nu_0)^2}{\eta_0^3} + \left[\kappa_{\dot{y}}\tau + \frac{r(1+e_0\cos\nu)^2}{\eta_0^3}\right]\frac{\partial\dot{\bar{\Omega}}}{\partial\bar{a}}\frac{\partial\xi_a}{\partial\nu}\frac{(1+e_0\cos\nu_0)^2}{\eta_0^3}$$

The elements of Φ for the computation of $\dot{z}$ are

$$\kappa_{\dot{z}} = -\dot{r}\cos(\nu+\omega_0+\dot{\bar{\omega}}\tau)\sin i_0 + r\sin(\nu+\omega_0+\dot{\bar{\omega}}\tau)(\dot{\nu}+\dot{\bar{\omega}})\sin i_0$$

$$\Phi_{31} = [\kappa_{\dot{z}}\tau - r\cos(\nu+\omega_0+\dot{\bar{\omega}}\tau)\sin i_0]\frac{\partial\dot{\bar{\Omega}}}{\partial\bar{a}}$$

$$\Phi_{32} = [\kappa_{\dot{z}}\tau - r\cos(\nu+\omega_0+\dot{\bar{\omega}}\tau)\sin i_0]\left[\frac{\partial\dot{\bar{\Omega}}}{\partial\bar{a}}\frac{\partial\xi_a}{\partial e} + \frac{\partial\dot{\bar{\Omega}}}{\partial\bar{a}}\frac{\partial\xi_a}{\partial\nu}\frac{\sin\nu_0}{\eta_0^2}(2+e_0\cos e_0) + \frac{\partial\dot{\bar{\Omega}}}{\partial\bar{e}}\right]$$

$$\Phi_{33} = \dot{r}\sin(\nu+\omega_0+\dot{\bar{\omega}}\tau) + r\cos(\nu+\omega_0+\dot{\bar{\omega}}\tau)(\dot{\nu}+\dot{\bar{\omega}}) + [\kappa_{\dot{z}}\tau - r\cos(\nu+\omega_0+\dot{\bar{\omega}}\tau)\sin i_0]\frac{\partial\dot{\bar{\Omega}}}{\partial\bar{a}}$$

$$\Phi_{34} = \kappa_{\dot{z}}$$

$$\Phi_{35} = [\kappa_{\dot{z}}\tau - r\cos(\nu+\omega_0+\dot{\bar{\omega}}\tau)\sin i_0]\frac{\partial\dot{\bar{\Omega}}}{\partial\bar{a}}\frac{\partial\xi_a}{\partial\omega}$$

$$\Phi_{36} = [\kappa_{\dot{z}}\tau - r\cos(\nu+\omega_0+\dot{\bar{\omega}}\tau)\sin i_0]\frac{\partial\dot{\bar{\Omega}}}{\partial\bar{a}}\frac{\partial\xi_a}{\partial\nu}\frac{(1+e_0\cos e_0)^2}{\eta_0^3}$$

The elements of Φ for the computation of x are

$$\Phi_{41} = \frac{r}{a_0} + \frac{a_0e_0\sin\nu}{\eta_0}\frac{\partial\dot{\bar{M}}}{\partial\bar{a}}\tau$$

$$\Phi_{42} = \frac{a_0e_0\sin\nu}{\eta_0}\left[\frac{\partial\dot{\bar{M}}}{\partial\bar{a}}\frac{\partial\xi_a}{\partial e} + \frac{\partial\dot{\bar{M}}}{\partial\bar{a}}\frac{\partial\xi_a}{\partial\nu}\frac{\sin\nu_0}{\eta_0^2}(2+e_0\cos e_0) + \frac{\partial\dot{\bar{M}}}{\partial\bar{e}}\right]\tau - a_0\cos\nu$$

$$\Phi_{43} = \frac{a_0e_0\sin\nu}{\eta_0}\left(\frac{\partial\dot{\bar{M}}}{\partial\bar{a}}\frac{\partial\xi_a}{\partial i} + \frac{\partial\dot{\bar{M}}}{\partial\bar{i}}\right)\tau$$

$$\Phi_{44} = 0$$

$$\Phi_{45} = \frac{a_0e_0\sin\nu}{\eta_0}\left(\frac{\partial\dot{\bar{M}}}{\partial\bar{a}}\frac{\partial\xi_a}{\partial\omega}\right)\tau$$

$$\Phi_{46} = \frac{a_0e_0\sin\nu}{\eta_0} + \frac{a_0e_0\sin\nu}{\eta_0}\frac{\partial\dot{\bar{M}}}{\partial\bar{a}}\frac{\partial\xi_a}{\partial\omega}\frac{(1+e_0\cos\nu_0)^2}{\eta_0^3}\tau$$

The elements of Φ for the computation of y are

$$\Phi_{51} = r\cos i_0\frac{\partial\dot{\bar{\Omega}}}{\partial\bar{a}}\tau + r\frac{\partial\dot{\bar{\omega}}}{\partial\bar{a}}\tau + \frac{r(1+e_0\cos\nu_0)^2}{\eta_0^3}\frac{\partial\dot{\bar{M}}}{\partial\bar{a}}\tau$$

$$\Phi_{52} = \frac{r\sin\nu}{\eta_0^2}(2+e_0\cos\nu) + r\cos i_0\left[\frac{\partial\dot{\bar{\Omega}}}{\partial\bar{a}}\frac{\partial\xi_a}{\partial e} + \frac{\partial\dot{\bar{\Omega}}}{\partial\bar{a}}\frac{\partial\xi_a}{\partial\nu}\frac{\sin\nu_0}{\eta_0^2}(2+e_0\cos e_0) + \frac{\partial\dot{\bar{\Omega}}}{\partial\bar{e}}\right]\tau + r\left[\frac{\partial\dot{\bar{\omega}}}{\partial\bar{a}}\frac{\partial\xi_a}{\partial e} + \frac{\partial\dot{\bar{\omega}}}{\partial\bar{a}}\frac{\partial\xi_a}{\partial\nu}\frac{\sin\nu_0}{\eta_0^2}(2+e_0\cos e_0) + \frac{\partial\dot{\bar{\omega}}}{\partial\bar{e}}\right]\tau + \frac{r(1+e_0\cos\nu_0)^2}{\eta_0^3}\left[\frac{\partial\dot{\bar{M}}}{\partial\bar{a}}\frac{\partial\xi_a}{\partial e} + \frac{\partial\dot{\bar{M}}}{\partial\bar{a}}\frac{\partial\xi_a}{\partial\nu}\frac{\sin\nu_0}{\eta_0^2}(2+e_0\cos e_0) + \frac{\partial\dot{\bar{M}}}{\partial\bar{e}}\right]\tau$$

$$\Phi_{53} = r\cos i_0\left(\frac{\partial\dot{\bar{\Omega}}}{\partial\bar{a}}\frac{\partial\xi_a}{\partial i} + \frac{\partial\dot{\bar{\Omega}}}{\partial\bar{i}}\right)\tau + r\left(\frac{\partial\dot{\bar{\omega}}}{\partial\bar{a}}\frac{\partial\xi_a}{\partial i} + \frac{\partial\dot{\bar{\omega}}}{\partial\bar{i}}\right)\tau + \frac{r(1+e_0\cos\nu_0)^2}{\eta_0^3}\left(\frac{\partial\dot{\bar{M}}}{\partial\bar{a}}\frac{\partial\xi_a}{\partial i} + \frac{\partial\dot{\bar{M}}}{\partial\bar{i}}\right)\tau$$

$$\Phi_{54} = r\cos i_0$$

$$\Phi_{55} = r + r\cos i_0 \frac{\partial \dot{\bar{\Omega}}}{\partial \bar{a}} \frac{\partial \xi_a}{\partial \omega}\tau + r\frac{\partial \dot{\bar{\omega}}}{\partial \bar{a}} \frac{\partial \xi_a}{\partial \omega}\tau + \frac{r(1+e_0\cos\nu_0)^2}{\eta_0^3} \frac{\partial \dot{\bar{M}}}{\partial \bar{a}} \frac{\partial \xi_a}{\partial \omega}\tau$$

$$\Phi_{56} = \frac{r(1+e_0\cos\nu)^2}{\eta_0^3} + r\cos i_0 \frac{\partial \dot{\bar{\Omega}}}{\partial \bar{a}} \frac{\partial \xi_a}{\partial \nu} \frac{(1+e_0\cos\nu_0)^2}{\eta_0^3}\tau + r\frac{\partial \dot{\bar{\omega}}}{\partial \bar{a}} \frac{\partial \xi_a}{\partial \nu} \frac{(1+e_0\cos\nu_0)^2}{\eta_0^3}\tau + r\frac{(1+e_0\cos\nu)^2}{\eta_0^3} \frac{\partial \dot{\bar{M}}}{\partial \bar{a}} \frac{\partial \xi_a}{\partial \nu} \frac{(1+e_0\cos\nu_0)^2}{\eta_0^3}\tau$$

The elements of Φ for the computation of z are

$$\Phi_{61} = -r\cos(\nu+\omega_0+\dot{\bar{\omega}})\sin i_0 \frac{\partial \dot{\bar{\Omega}}}{\partial \bar{a}}\tau$$

$$\Phi_{62} = -r\cos(\nu+\omega_0+\dot{\bar{\omega}})\sin i_0 \left[\frac{\partial \dot{\bar{\Omega}}}{\partial \bar{a}} \frac{\partial \xi_a}{\partial e} + \frac{\partial \dot{\bar{\Omega}}}{\partial \bar{a}} \frac{\partial \xi_a}{\partial \nu} \frac{\sin\nu_0}{\eta_0^2}(2+e_0\cos e_0) + \frac{\partial \dot{\bar{\Omega}}}{\partial \bar{e}}\right]\tau$$

$$\Phi_{63} = r\sin(\nu+\omega_0+\dot{\bar{\omega}}) - r\cos(\nu+\omega_0+\dot{\bar{\omega}})\sin i_0 \left(\frac{\partial \dot{\bar{\Omega}}}{\partial \bar{a}} \frac{\partial \xi_a}{\partial i} + \frac{\partial \dot{\bar{\Omega}}}{\partial \bar{i}}\right)\tau$$

$$\Phi_{64} = -r\cos(\nu+\omega_0+\dot{\bar{\omega}})\sin i_0$$

$$\Phi_{65} = -r\cos(\nu+\omega_0+\dot{\bar{\omega}})\sin i_0 \frac{\partial \dot{\bar{\Omega}}}{\partial \bar{a}} \frac{\partial \xi_a}{\partial \omega}\tau$$

$$\Phi_{66} = -r\cos(\nu+\omega_0+\dot{\bar{\omega}})\sin i_0 \frac{\partial \dot{\bar{\Omega}}}{\partial \bar{a}} \frac{\partial \xi_a}{\partial \nu} \frac{(1+e_0\cos\nu_0)^2}{\eta_0^3}\tau$$

References

[1] Vallado, D. A., *Fundamentals of Astrodynamics and Applications*, 2nd ed., Space Technology Library, Microcosm, Segundo, CA, and Kluwer Academic, Dordrecht, The Netherlands, 2001.

[2] Sabol, C., Burns, R., and McLaughlin, C. A., "Satellite Formation Flying Design and Evolution," *Journal of Spacecraft and Rockets*, Vol. 38, No. 2, Mar.–Apr. 2001, pp. 270–278.

[3] Lovell, T. A., and Tragesser, S. G., "Analysis of the Reconfiguration and Maintenance of Close Spacecraft Formations," 13th AAS/AIAA Space Flight Mechanics Conference, Ponce, Puerto Rico, American Astronautical Society Paper 03-139, Feb. 2003.

[4] Inalhan, G., Tillerson, M., and How, J. P., "Relative Dynamics and Control of Spacecraft Formations in Eccentric Orbits," *Journal of Guidance, Control, and Dynamics*, Vol. 25, No. 1, Jan.–Feb. 2002, pp. 48–59.

[5] Schaub, H., "Relative Orbit Geometry Through Classical Orbit Element Differences," *Journal of Guidance, Control, and Dynamics*, Vol. 27, No. 5, Sept.–Oct. 2004, pp. 839–848.

[6] Broucke, R. A., "Solution of the Elliptic Rendezvous Problem with the Time as Independant Variable," *Journal of Guidance, Control, and Dynamics*, Vol. 26, No. 4, July–Aug. 2003, pp. 615–621.

[7] Zanon, D. J., and Campbell, M. E., "Optimal Planner for Spacecraft Formations in Elliptical Orbits," *Journal of Guidance, Control, and Dynamics*, Vol. 29, No. 1, Jan.–Feb. 2006, pp. 161–171.

[8] Lane, C., and Axelrad, P., "Formation Design in Eccentric Orbits Using Linearized Equations of Relative Motion," *Journal of Guidance, Control, and Dynamics*, Vol. 29, No. 1, Jan.–Feb. 2006, pp. 146–160.

[9] Melton, R. G., "Time-Explicit Representation of Relative Motion Between Elliptical Orbits," *Journal of Guidance, Control, and Dynamics*, Vol. 23, No. 4, July–Aug. 2000, pp. 604–610.

[10] Schweighart, S. A., and Sedwick, R. J., "High-Fidelity Linearized J_2 Model for Satellite Formation Flight," *Journal of Guidance, Control, and Dynamics*, Vol. 25, No. 6, Nov.–Dec. 2002, pp. 1073–1080.

[11] Schweighart, S. A., and Sedwick, R. J., "Cross-Track Motion of Satellite Formations in the Presence of J_2 Disturbances," *Journal of Guidance, Control, and Dynamics*, Vol. 28, No. 4, July–Aug. 2005, pp. 824–826.

[12] Kechichian, J. A., "Motion in General Elliptic Orbit with Respect to a Dragging and Precessing Coordinate Frame," *Journal of the Astronautical Sciences*, Vol. 46, No. 1, 1998, pp. 25–45.

[13] Bate, R. R., Mueller, D. D., and White, J. E., *Fundamentals of Astrodynamics*, Dover, New York, 1971.

[14] Gim, D.-W., and Alfriend, K. T., "State Transition Matrix of Relative Motion for the Perturbed Noncircular Reference Orbit," *Journal of Guidance, Control, and Dynamics*, Vol. 26, No. 6, Nov.–Dec. 2003, pp. 956–971.

[15] Schaub, H., and Junkins, J. L., *Analytical Mechanics of Space Systems*, AIAA Education Series, AIAA, Reston, VA, 2003.

[16] Brouwer, D., "Solution of the Problem of Artificial Satellite Theory Without Drag," *Astronomical Journal*, Vol. 64, No. 1274, Nov. 1959, pp. 378–397.

[17] Schaub, H., and Alfriend, K. T., "J_2 Invariant Relative Orbits for Spacecraft Formations," *Celestial Mechanics and Dynamical Astronomy*, Vol. 79, No. 2, Feb. 2001, pp. 77–95.